Title:

A comprehensive catalogue of predicted functional upstream open reading frames numbering hundreds of thousands.

Patrick McGillivray, Russell Ault, Mayur Pawashe, Rob Kitchen, Suganthi Balasubramanian, Mark Gerstein

Abstract

Upstream open reading frames (uORFs), are associated with translational regulation of downstream coding sequences. The translation of a uORF latent in an mRNA transcript, is thought to modify the translation of coding sequences in that same transcript, by modifying ribosome localization. Not all uORFs are thought to be active in such a process. It represents a challenge to estimate the impact and scope of the role uORFs play in regulation of translation.

We use the GENCODE annotation of the human genome, to circumscribe the universe of all possible translated uORFs. This universe includes over one million unique uORFs. We compare patterns of structure in these uORFs, to the structure of uORFs labeled as translated in experiment. This comparison allows us to catalog a population of uORFs that likely undergo translation. This population numbers 188 802. Eleven thousand protein coding genes include at least one likely translated uORF.

This is a substantially larger population uORFs, than has previously been associated with active translation. It suggests the translation of uORFs, is a widespread phenomenon, with considerable impact on the translational landscape.

Our catalog of uORFs, allows researchers to test their hypotheses regarding the role of upstream open reading frames, in health and disease.

Intro

Upstream open reading frames (uORFs) consist of a start codon in the 5' untranslated region of a gene (UTR), and an associated stop codon appearing before the stop codon of the main coding sequence (CDS). The uORF may begin and end before the main gene coding sequence. Alternatively, if the upstream reading frame is out of frame with the CDS, it may overlap with the CDS [Figure 1.A]. uORFs are latent in mRNA transcripts, and may undergo partial or complete translation.

Initial survey of the human genome, identified uORFs contained in approximately 10% of mRNA transcripts(1). More recent analyses broaden estimates of prevalence, with identification of uORFs in association with nearly half of all mRNA transcripts(2). The discovery that many uORFs utilize near-cognate start codons, rather than the canonical ATG start codon, has broadened estimates of uORF prevalence still further(3–6).

Study of uORF translation and function, was historically limited to the experimental evaluation of individual uORFs(7,8), with no genome-scale approach to identifying translated uORFs. The advent of ribosome profiling studies, has allowed for the identification of a large population of

uORFs known to undergo translation(4,9,10). Ribosome profiling studies that arrest the ribosome at translation initiation, allow for the identification of translation initiation sites to within a few nucleotides. This mapping of translation initiation is sufficient for association between ribosomes and particular start codons and reading frames (11–13).

At the same time as ribosome profiling studies have allowed for large-scale identification of upstream open reading frames, there has been expansion in knowledge of the functional role of uORFs. Upstream open reading frames, have generally been thought to suppress translation of downstream genes(8,14–18). The molecular mechanisms for modification of translation are varied, and include leaky-scanning of uORFs by ribosomes, translation reinitiation subsequent to uORF translation, and ribosome-stalling on uORFs. These mechanisms have been uncovered in some detail (3,19,20). Apart from increases and decreases in a single protein product, differential translation of multiple protein products may occur in consequence to a uORF(21). There may even be additional direct effect of translated products between uORF and CDS, as has been observed in dual-coding genes(22).

From these studies, it is important to note, that a uORF may increase translation of the downstream CDS or decrease translation of the downstream CDS, according to genomic and epigenomic context. Related to a differential effect of uORFs on CDS translation, depending on context, the study of translation in stress conditions, has revealed a differential function for uORFs in stressed cells, compared with non-stressed controls(23–28).

Interest in the study of the function of upstream open reading frames has also increased related the discovery of short open reading frames, encoding short functional peptides. These functional peptides from short open reading frames, may be differentiated from upstream open reading frames: uORFs are thought to have primarily regulatory control. (29–31) However, it is a strong possibility that many upstream open reading frames, once thought to only have regulatory impact, will be re-evaluated for the possibility that they encode functional protein products.

Discovery of the function of uORFs, is predicated on identification of uORFs that are translated. For this reason, we took interest in the identification of translated uORFs in humans. We hypothesized that the total universe of translated upstream open reading frames, is much larger than that identified through ribosome profiling experiments. In other words, perhaps ribosome profiling experiments are sensitive in identifying translated uORFs, but not specific.

Researchers have recently explored this hypothesis in other species (32,33), and ribosome profiling read attributes, such as ribosome profiling reading frame, have been used in humans to identify novel translation products(34,35) These areas of study have proven productive. In these non-human and human studies, novel translated CDSs and uORFs were identified, numbering in the thousands.

For our investigation of the prevalence of translated upstream open reading frames in humans, we began by performing a computational scan of the GENCODE genome annotation(36). We searched for uORFs associated with protein coding genes. All the possible uORFs beginning

either with ATG, or a near-cognate start codon, were identified (all single nucleotide variants of the canonical ATG). This scan yields a universe of all possible uORFs, numbering nearly 1.3 million.

We do not expect that all uORFs identified in a genome-wide scan are functional. For this reason, we sought means to separate translated uORFs, from uORFs with a low chance translation. In order to effect this identifcication of functional uORFs, we studied the human ribosome profiling experiments of three research groups – Lee et al. 2012, Fritsch et al. 2012, and Gao et al. 2014 (11–13). Each of these three experiments uses translational inhibitors that arrest the translating ribosome at the first peptide bond. This arrest of translation at initiation, allows for the identification of translated upstream open reading frames to high precision.

uORFs in our computational set, that displayed considerable similarity to known translated uORFs, we predicted to be translated and functional. We validate our predicted uORFs, using statistical analyses, by examining the of individual genotype on parameters related to uORF translation.

Following examination efficacy of our method, we demonstrate applications of our large set of predicted uORFs. Specifically, we intersect the predictions we generate, with known variants from tissue-matched tumor samples(37), and the 1000 Genomes project's database of human variation(38). In this way, we identify circumstances where human genomic variation and mutation, are likely to have functional impact mediated by uORFs.

The set of uORFs that we predict are likely translated and functional, extends scope far beyond those identified in ribosome profiling experiments. Through our study, we predicted that there exist hundreds of thousands of translated, functional uORFs – two orders of magnitude higher, than in other studies. We hope that our procedure for identifying translated uORFs, will be of use to other scientists in their effort to understand uORF function in health and disease.

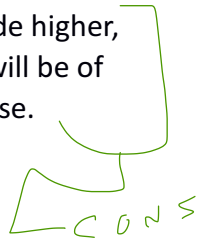

Methods:

Extracting uORFs from GENCODE:

uORFs were extracted from the v19 of the GENCODE annotation of the human genome(36). uORFs were defined as a start codon within the 5'UTR, and a downstream stop codon before the end of the CDS. All three possible reading frames were examined. ATG, and near cognate start codons were included in this search [ATG, TTG, GTG, CTG, AAG, AGG, ACG, ATA, ATT, ATC].

Ribosome profiling experiments as a reference set:

The ribosome profiling experiments of Lee et al. (2012), Fritsch et al. (2012) and Gao et al. (2015), were used to obtain an experimentally validated set of translated upstream open reading frames [Figure 1.B]. These studies identify translation initiation sites (TIS), through treatment of human cell lines with antibiotic translation inhibitors. These treatments reliably halt translation, in predictable proximity to the start codon (12-13 nucleotides downstream). As such, these experiments provide us with high resolution information about translation initiation sites in the human genome.

We employed the read alignments and identification of the translation initiation sites, as provided by these three groups of researchers. Each group ultimately expressed their results as positional coordinates for uORF start codons, with corresponding transcripts identified by RefSeqID. We mapped the RefSeqIDs provided in these papers, to corresponding GENCODE Ensembl IDs. This mapping provides position information in the global positioning coordinates of the GENCODE annotation.

The cell lines, treatment protocols, and TIS identification mechanism employed by each of these three research groups is summarized in Table 1.

Study	***Cell line***	***Treatment protocol***	***TIS identification***
Fritsch et al.	THP1	cyclohexamide + puromycin	Novalign + neural network
Lee et al.	HEK293	lactidomycin	Bowtie + threshold on nucleotide resolution read counts
Gao et al.	HEK293	cyclohexamide + lactimidomycin + puromycin	TopHat + ZTNB model

Literature review of translated human uORFs:

In addition to ribosome profiling studies, confirmed translated uORFs were obtained from the biomedical literature(8,39,40). uORFs studied in humans that displayed functionality (demonstrated regulation of the CDS product) were added to the set of positive uORFs. In total, 33 uORFs, associated with 33 separate genes, were included from this literature review.

Cleansing the data set, by removal of N-terminal extensions and aTISs, and isolation of unique transcript IDs:

Reading frames labeled as uORFs in experiment, but without a stop codon before the stop codon of the CDS, contain the complete CDS sequence. These N-terminal extensions of the CDS sequence, may have some of the functional activity of the primary gene protein product, and were removed from the data set. In addition, any uORF start codon that is annotated as an alternative translation initiation sites (aTISs) for the CDS, was also removed from the data set.

Multiple transcript IDs, may share identical chromosomal coordinates. In order to avoid over-counting, only one transcript ID was included for a given set of chromosomal coordinates. This selection was made randomly, from among transcripts with identical chromosomal coordinates.

Positive, neutral, and unlabeled data sets:

uORFs were divided into three separate sets, according to their experimental translation status:

Positive: uORFs identified as translated in two or more ribosome profiling experiments, or through literature review.
Neutral: uORFs identified as translated in not more than one ribosome profiling experiment.
Unlabeled: uORFs that were not identified as translated in any ribosome profiling experiment, or through literature review.

Extraction of attributes associated with uORFs:

In order to determine what features make a uORF more likely to be transcribed (classified as positive), feature data was extracted for each uORF. 89 features were used. Details relating to the extraction and calculation of each of these features, is included in *Methods Supplement*.

Feature discretization:

The minimum description length principle (MDLP) algorithm was used to discretize each uORF attribute(41). The MDLP algorithm discretizes data, while optimizing bin size according to a information theoretic principle. MDLP discretization was implemented using the 'discretization' package available for R (http://cran.r-project.org/web/packages/discretization/index.html).

Some included features showed little variability among uORFs. Accordingly, these features became uniform upon discretization. For this reason, these features were be rejected from the analysis.

Prioritization of feature data:

For each included feature, the distribution for that feature was compared between positive and unlabeled uORFs. This comparison was completed using the kolmogorov-smirnov (KS) statistic. A greater KS statistic, indicates a greater difference between the distributions for that feature. The KS statistic was thus used as a proxy for the ability of that attribute, to distinguish between positive and unlabeled features.

Classifying uORFs, according to attributes:

Using discretized feature data, the probability distribution for each attribute was used to distinguish between positive uORFs and unlabeled uORFs. For a given uORF, we determined if the attributes of that uORF were consitent with a translated uORF, according to the following algorithm:

$$P_{pos}\prod_{i=\{1\ldots89\}}p(A_i|pos) == p_{pos}$$
$$P_{neg}\prod_{i=\{1\ldots89\}}p(A_i|unl) == p_{neg}$$

With

$$P_{pos} = 0.61$$
$$P_{neg} = 1 = P_{pos}$$

This formulation corresponds to a Naive-Bayes machine learning algorithm applied to positive and unlabeled examples(42). P_{pos} is the prior probability associated with positive uORFs, P_{neg} is the prior probability associated with negative uORFs. A_i is the value of a given attribute, such that $p(A_i|pos)$, and $p(A_i|unl)$ represent the frequency of that attribute value among the positive, and unlabeled sets respectively. p_{pos} represents the probability the uORF is positive. p_{neg} represents the probability the uORF is positive.

Model validation:

To validate our model, we serially trained our model on two of three ribosome profiling data sets, using the model to extract the third ribosome profiling data set from among the unlabeled examples. The success of these differentially trained models, is expressed as ROC curves, with area under the curve (AUC) calculated for each curve.

In order to estimate the effect on protein level, attributable to natural variation affecting predicted translated uORFs, we intersected our set of predicted translated uORFs, with ribosome quantatative trait loci (rQTL), and protein level according to gene. This protein level and rQTL data, was obtained from the supplemental information of Battle et al. 2015(43). Genotype information per individual, was obtained from the 1000 Genomes project.

Natural variation interrupting predicted positive uORFs:

SNPs obtained from the 1000 Genomes project, were intersected with start codons for our set of positive uORFs. This allows for measurement of the comparative frequency of mutation of uORF start codons, suggestive of evolutionary conservation. It also allows for identification of SNPs interrupting uORF start codons that are also associated with differential disease susceptibility. Associations of disease susceptibility for specific SNPs, was evaluated via PubMed database search via RefSNP (rs) ID.

Cancer mutation interrupting predicted positive uORFs:

The study of Alexandrov et al. 2012(37) provides a set of exomic somatic mutations according to patient sample, and cancer type. We intersected this database of cancer mutation, with the start codons of our predicted positive uORFs. This allowed for estimation of the frequency with which start codons are interrupted in cancer, according to cancer type and according to uORF start codon. Patterns of function in genes affected by mutation of uORFs in cancer, was assessed via the GO genome annotation database(44). Overrepresented GO terms were identified, with overrepresentation assessed via the hypergeometric statistical test, with multiple testing correction via Benjamini & Hochberg's FDR correction(45). Networks between GO terms, were constructed using the Cytoscape package BiNGO(46).

Results:

The search of the GENCODE genome annotation, for the universe of all possible uORFs, yielded 1 270 265 unique uORFs. Within this large set, we isolated the subset of uORFs found to be translated in the studies of Lee et al. 2012, Fritsch et al. 2012, and Gao et al. 2015 [Figure 1.C]. We further stratified this set of translated uORFs, according to shared representation of uORFs among the three studies. uORFs identified in the intersection between two or more of these studies, were used as the reference standard for translated uORFs. This intersection also helps to control for false positives, and to control for differences in experimental procedure and tissue specificity (HEK293 vs. THP-1). Literature review, yielded 33 additional examples of translated uORFs, that were also included in the set of positive, translated uORFs.

Overlap between the three ribosome profiling experiments was found to be low, with pairwise intersections of 12.2% (Gao ∩ Fritsch), 9.2% (Gao ∩ Lee), and 9.8% (Lee ∩ Fritsch), with the number of uORFs shared between all three sets representing only 3.3% of uORFs identified in these studies.

The relative representation of start codons identified in ribosome profiling experiments, is noteworthy for the prevalence of both CTG (28.2%) and ATG (46.1%) start codons. These start codons represent the majority (74.3%) of start codons found in these ribosome profiling studies. In intersection between ribosome profiling studies, CTG (30.5%) and ATG (34.6%) continue to represent the majority of start codons (65.1%) [Figure 1.C.]. Representation of every near-cognate start codon was found in intersections between studies, with the exception of AAG and AGG.

We next followed the procedure outlined in figure 2.A, in an effort to distill uORFs that are likely to be translated, from those identified via genome-wide scan. To begin this process, three categories of uORF were delineated, based on observed translation in experimental study:

1. positive uORFs – translated in at least two ribosome profiling experiments or via literature review.
2. neutral uORFs – translated in only one ribosome profiling study.
3. unlabeled uORFs – not translated in ribosome profiling studies, or literature review.

Distributions of attributes for positive, translated uORFs, were compared with distributions of those same attributes as observed in the set of unlabeled, computationally derived uORFs [Figure 2.B.]. The usefulness of individual attributes in making this comparison, was measured using the kolmogorov smirnov (KS) statistical test. A higher KS statistic, indicates greater difference between the attribute distributions, suggesting that the attribute is of greater utility in identifying translated uORFs. The KS statistic and corresponding p-value, for each of the 89 attributes assessed in this study, is provided in Table 2. The top 10 attributes, listed according to magnitude of KS statistic, are given in Figure 2.C.

The discretized attributes of positive and unlabeled sets of uORFs, were used to build a statistical classifier, within a Naive-Bayes framework. This classifier predicts translated uORFs, through examination of the totality of attributes associated with an individual uORF.

The result of application of the classifier is shown in figure 3.A. The percentage of positive examples, that are ultimately retained as likely translated is 76.8% [590/768], 67.1% of neutral uORFs are classified as likely translated [2379/3543], and 14.7% of unlabeled uORFs are likely translated [185833/1265954].

The overall number of uORFs classified as likely translated, is *188 802*, representing 14.9% of computationally identified uORFs [188802/1270265]. 140 668 (75.5%) of these uORFs lie entirely upstream of the CDS, throughout their length. 48 134 (25.5%) of these uORFs are out-of-frame with the CDS, and overlap with the CDS. A complete list of upstream open reading frames identified as likely translated is provided in *Results Supplement.*

As validation of our technique for distinguishing between positive and unlabeled upstream open reading frames, we serially excluded one of the three ribosome profiling experiments from the positive training set, including that set among the unlabeled examples. Retrieval of the excluded set, then functions as a measure of the accuracy and generalizability of our method. The result of this validation procedure is shown in Figure 3.B. The ROC curve for the retrieval of each ribosome profiling set is given. The AUC for each of these ROC curves, is similar. 0.82, 0.79, and 0.77 for the retrieval of Lee, Gao, and Fritsch uORFs respectively.

The proportion of uORFs ultimately identified as positive, from each ribosome profiling study, is shown in Figure 3.C. The results were similar for each of the ribosome profiling experiments, at approximately 70% in each case (72% of Gao, 71% of Lee, 70% of Fritsch).

The distribution of start codons for predicted translated uORFs, in comparison to the computational set, is shown in Figure 3.D. There are a large number of CTG start codons in the computationally derived set (19.3%), and the greatest number of predicted positive uORFs are also initiated with a CTG start codon 11.8%. Similarly, TTG (9.9%) and GTG (12.4%) have high prevalence in the computationally derived set, and this is reflected in the predicted translated set (13.2% and 19.3% respectively). ATG has a lower comparative prevalence in both the computationally derived set, and predicted set (6.7% and 8.2% respectively).

As an application of our list of predicted positive uORFs, we intersected our predicted positive uORFs, with germline variants from the 1000 Genomes project. Figure 4.A shows the frequency with which predicted positive start codons are broken by germline variants, normalized for population start codon frequency. The ATG start codon is relatively conserved, among start codons. It is rarely interrupted by human variants (relative rate (RR) 0.03, compared to the most frequently interrupted start codon). The CTG start codon, although more prevalent among predicted positive uORFs, is broken relatively frequently by natural human variants (RR 0.52). Human germline variants that intersect with high scoring uORFs, and disease associations identified via literature review, are listed in Table 3.

An analysis of the interruption of predicted positive uORFs, was applied to somatic mutations across cancer types. This analysis is shown in figure 4.B. CTG is the most commonly interrupted start codon in these combined cancers. ATG is interrupted at a RR of 0.25 in comparison to CTG. Exomic cancer mutations breaking the highest scored uORFs, are listed in Table 4.

In order to evaluate the frequency with which uORFs are interrupted by mutation in cancer, the proportion of positive uORFs interrupted by mutation was calculated for each cancer type. This analysis is shown in Figure 4.C. This proportion of positively scored uORFs to negative scored uORFs, is near consistent across cancer types, ranging from a low of 8:1 for acute lymphoblastic leukemia, to a high of 20:1 for pancreatic cancer. The between group differences for interrupted predicted translated uORFs are significant (chi-square = 45, p-value = <<0.001). Networks of GO terms were constructed, for those genes associated with the mutation of predicted translated uORFs in cancer [Figure 4.D.]. Three networks of overrepresented GO terms remain, following correction for statistical significance, and multiple testing. These networks are associated with cellular death, immune modulation, and tissue morphogenesis.

Using our inventory of likely translated uORFs, we further explored the possible relationship between uORFs, and the regulation of downstream protein coding genes. We examined the effect of uORF interruption on ribosome occupancy and protein level.

Protein level was assessed through comparison of gene resolution protein levels in individuals with start codon interrupting SNPs, compared to individuals without these variants [Figure 4.E.]. In cases where few of the 47 individuals assessed, are in possession of the start codon interrupting variant, this method is underpowered to assess the effect on protein level. However, for those genes where this natural experiment provides close to the ideal assignment ratio of 23 individuals per group, we a see a definite trend to decreased protein levels. This decrease is statistically significant at the limit of >22 individuals per group.

To examine the effect of uORFs on ribosome occupancy, we answered the question – how many rQTLs that interrupt a uORF start codon, interrupt a positively scored start codon? Figure 4.F. displays the results of such an analysis, showing significant enrichment among this set of rQTLs, for rQTLs interrupting positively scored start codons. While the effect we would expect due to random mutation is 14.9%, we observed that 48% of these rQTLs (21/44) interrupt positively scored start codons.

Discussion:

In this study, we were able to identify 188 802 likely translated upstream open reading frames, from a global set of 1 270 265 unique uORFs identified in the human genome.

The number of uORFs identified as likely translated is remarkable, in comparison to other studies of this topic. No other study examining the global translation of uORFs, suggests that the

number of translated uORFs numbers more than a few thousand. Indeed, our large number of predicted sites of translation alone, may cause other investigators to doubt our result.

In relation to this result – it is with interesting to note low levels of overlap, between ribosome profiling studies. 3.3% shared overlap, suggests that these ribosome profiling studies include either a significant proportion of false positives –- low specificity -- or a significant proportion of false negatives -- low sensitivity. Our result suggests that ribosome profiling studies provide a low sensitivity to detect the translation initiation sites of uORFs.

The frequency of alternative uORF start codons, suggests an additional explanation for the abundance of likely translated uORFs. ATG is the most common uORF start codon in the ribosome profiling studies examined in this study (46.1%). However, it is only the fourth most common uORF start codon identified computationally, and 5th most common predicted positive uORF start codon. The high affinity of ATG as a translation initiation site, likely leads to its over-representation in ribosome profiling studies. Conversely, near-cognate start codons with lower affinity, may not meet thresholds for identification in ribosome profiling studies. However, near-cognate start codons, due to their overall abundance, may ultimately have the greatest functional impact on the landscape of translation.

Finally, we used the intersection of three ribosome profiling studies, to form a gold-standard known translated set of translated uORFs. This suggests a further explanation for low overlap between ribosome profiling studies, and the remarkably high number of translated uORFs we predict. Our use of an intersection between ribosome profiling studies, provides some control against tissue specific results (both human embryonic kidney, and human monocytic cell lines were examined). It also provides some control against differences experimental protocol. Just as protein levels vary widely across cell-type(47), it is not unreasonable to imagine that the translation of uORFs varies greatly in different cell types, and different cellular conditions. This is also suggested by the large number of studies that have demonstrated the differential translation from uORF start codons, in stress conditions compared to control.

Confidence in our result is gained, through use of a robust cross-validation mechanism. This mechanism is based on false-negative retrieval from independent datasets -- not just fractions of datasets. This validation shows that the procedure we follow is sufficiently generalized. Training on two of three data sets, with retrieval of the third data set, shows near equivalent high accuracy retrieval in each case (ROC AUC ~0.7) [Figure 3.B.].

Further confidence in the validity of our result is gained through its application. The use of our catalog of likely translated upstream open reading frames, in intersection with human germline variants, suggests a number of sites where the creation or destruction of uORFs, is likely to alter protein levels. This may in turn lead to disease susceptibility. These sites should be of interest to other research groups, particularly as the number of sequencing experiments that include non-coding regions increases.

The application of our results to exomic cancer mutation data, identifies locations where the mutation of uORFs, may contribute to the pathogenesis of cancer. GO terms, associated with the mutation of predicted translated uORFs in cancer, appear to correspond to essential domains of cancer pathogenesis: tissue morphogenesis, cellular survival, and immunologic response. Mutation sites that we identify, may result in carcinogenesis, via defect in regulation of translation. Mutation of uORFs, may either up-regulation of oncogenes, or down-regulation of tumor suppressor genes. In this way, our work could help broaden knowledge of the role of uORFs in cancer, beyond recently identified individual examples(48).

The combination of our results, with the study of ribosome occupancy (rQTLs), and gene-resolution proteomics, yields a further validation of the method. It is seen that a large majority of rQTLs that intersect uORF start codons, may owe their significance to the uORFs that they modify. Our additional observation, that the interruption of a predicted positive uORF, has significant impact on downstream protein level, also suggests validity of our predictions. In this case, it is also of interest, that the overall effect of uORF interruption, appears to be a decrease in the downstream protein level. This is contrary to common view that uORFs act as translational repressors. Mechanisms have been studied, where uORFs act to up-regulate the presence of a downstream coding sequence (e.g. leaky-scanning). Our analysis would appear to suggest that this effect is a possibly common consequence for upstream open reading frames. However, we note that this natural experiment is at a minimum threshold of statistical power, and would benefit from repeat observation in a larger cohort.

These applications of our results, suggest exciting avenues for future research. Our results offer a broad and validated catalog of uORFs. We hope that catalog can serve as a point of reference for other researchers, towards investigation of the function of uORFs, in meaningful context to areas of personal expertise and interest.

Bibliography:

1. Kozak M. An analysis of 5’-noncoding sequences from 699 vertebrate messenger RNAs. Nucleic Acids Res [Internet]. 1987 [cited 2016 Aug 16];15(20):8125–48. Available from: http://nar.oxfordjournals.org/lookup/doi/10.1093/nar/15.20.8125
2. Kochetov A V., Sarai A, Rogozin IB, Shumny VK, Kolchanov NA. The role of alternative translation start sites in the generation of human protein diversity. Mol Genet Genomics [Internet]. 2005 Jul 15 [cited 2016 Aug 16];273(6):491–6. Available from: http://link.springer.com/10.1007/s00438-005-1152-7
3. Ingolia NT, Lareau LF, Weissman JS. Ribosome Profiling of Mouse Embryonic Stem Cells Reveals the Complexity and Dynamics of Mammalian Proteomes. Cell. 2011;147(4):789–802.

4. Ingolia NT, Ghaemmaghami S, Newman JRS, Weissman JS. Genome-wide analysis in vivo of translation with nucleotide resolution using ribosome profiling. Science [Internet]. 2009 Apr 10 [cited 2016 Aug 16];324(5924):218–23. Available from: http://www.ncbi.nlm.nih.gov/pubmed/19213877

5. Ivanov IP, Loughran G, Atkins JF. uORFs with unusual translational start codons autoregulate expression of eukaryotic ornithine decarboxylase homologs. Proc Natl Acad Sci [Internet]. 2008 Jul 22 [cited 2016 Aug 23];105(29):10079–84. Available from: http://www.pnas.org/cgi/doi/10.1073/pnas.0801590105

6. Ivanov IP, Firth AE, Michel AM, Atkins JF, Baranov P V. Identification of evolutionarily conserved non-AUG-initiated N-terminal extensions in human coding sequences. Nucleic Acids Res [Internet]. 2011 May 1 [cited 2016 Aug 17];39(10):4220–34. Available from: http://nar.oxfordjournals.org/lookup/doi/10.1093/nar/gkr007

7. Kozak M. Point mutations define a sequence flanking the AUG initiator codon that modulates translation by eukaryotic ribosomes. Cell [Internet]. 1986 Jan [cited 2016 Aug 17];44(2):283–92. Available from: http://linkinghub.elsevier.com/retrieve/pii/0092867486907622

8. Calvo SE, Pagliarini DJ, Mootha VK. Upstream open reading frames cause widespread reduction of protein expression and are polymorphic among humans. Proc Natl Acad Sci [Internet]. 2009 May 5 [cited 2016 Aug 16];106(18):7507–12. Available from: http://www.pnas.org/cgi/doi/10.1073/pnas.0810916106

9. Brar G a, Weissman JS. Ribosome profiling reveals the what, when, where and how of protein synthesis. Nat Rev Mol Cell Biol [Internet]. 2015;16(11):651–64. Available from: http://www.ncbi.nlm.nih.gov/pubmed/26465719

10. Ingolia NT. Ribosome profiling: new views of translation, from single codons to genome scale. Nat Rev Genet [Internet]. 2014 Jan 28 [cited 2016 Aug 17];15(3):205–13. Available from: http://www.nature.com/doifinder/10.1038/nrg3645

11. Gao X, Wan J, Liu B, Ma M, Shen B, Qian S-B. Quantitative profiling of initiating ribosomes in vivo. Nat Methods [Internet]. 2014 Dec 8 [cited 2016 Aug 17];12(2):147–53. Available from: http://www.nature.com/doifinder/10.1038/nmeth.3208

12. Fritsch C, Herrmann A, Nothnagel M, Szafranski K, Huse K, Schumann F, et al. Genome-wide search for novel human uORFs and N-terminal protein extensions using ribosomal footprinting. Genome Res [Internet]. 2012 Nov 1 [cited 2016 Aug 17];22(11):2208–18. Available from: http://genome.cshlp.org/cgi/doi/10.1101/gr.139568.112

13. Lee S, Liu B, Lee S, Huang S-X, Shen B, Qian S-B. Global mapping of translation initiation sites in mammalian cells at single-nucleotide resolution. Proc Natl Acad Sci [Internet]. 2012 Sep 11 [cited 2016 Aug 17];109(37):E2424–32. Available from: http://www.pnas.org/cgi/doi/10.1073/pnas.1207846109

14. Johnstone TG, Bazzini AA, Giraldez AJ, Abràmofff M, Magalhães P, Ram S, et al. Upstream ORFs are prevalent translational repressors in vertebrates. EMBO J [Internet]. 2016 Apr 1 [cited 2016 Aug 17];35(7):706–23. Available from: http://emboj.embopress.org/lookup/doi/10.15252/embj.201592759

15. Somers J, Pöyry T, Willis AE. A perspective on mammalian upstream open reading frame function. Int J Biochem Cell Biol. 2013;45(8):1690–700.

16. Meijer HA, Thomas AAM. Control of eukaryotic protein synthesis by upstream open reading frames in the 5'-untranslated region of an mRNA. Biochem J [Internet]. 2002 Oct 1 [cited 2016 Aug 17];367(Pt 1):1–11. Available from: http://www.ncbi.nlm.nih.gov/pubmed/12117416

17. Barbosa C, Peixeiro I, Romão L. Gene expression regulation by upstream open reading frames and human disease. PLoS Genet [Internet]. 2013 [cited 2016 Aug 17];9(8):e1003529. Available from: http://www.ncbi.nlm.nih.gov/pubmed/23950723

18. Morris DR, Geballe AP. Upstream Open Reading Frames as Regulators of mRNA Translation. Mol Cell Biol [Internet]. 2000 Dec 1 [cited 2016 Aug 17];20(23):8635–42. Available from: http://mcb.asm.org/cgi/doi/10.1128/MCB.20.23.8635-8642.2000

19. Sonenberg N, Hinnebusch AG. Regulation of translation initiation in eukaryotes: mechanisms and biological targets. Cell [Internet]. 2009 Feb 20 [cited 2016 Aug 30];136(4):731–45. Available from: http://www.ncbi.nlm.nih.gov/pubmed/19239892

20. Hinnebusch AG, Ivanov IP, Sonenberg N, Hinnebusch AG, Kozak M, Starck SR, et al. Translational control by 5'-untranslated regions of eukaryotic mRNAs. Science [Internet]. 2016 Jun 17 [cited 2016 Aug 17];352(6292):1413–6. Available from: http://www.ncbi.nlm.nih.gov/pubmed/27313038

21. Chua JJE, Schob C, Rehbein M, Gkogkas CG, Richter D, Kindler S, et al. Synthesis of two SAPAP3 isoforms from a single mRNA is mediated via alternative translational initiation. Sci Rep [Internet]. 2012 Jul 2 [cited 2016 Aug 16];2:277–98. Available from: http://www.nature.com/articles/srep00484

22. Bergeron D, Lapointe C, Bissonnette C, Tremblay G, Motard J, Roucou X. An Out-of-frame Overlapping Reading Frame in the Ataxin-1 Coding Sequence Encodes a Novel Ataxin-1

Interacting Protein. J Biol Chem [Internet]. 2013 Jul 26 [cited 2016 Aug 17];288(30):21824–35. Available from: http://www.jbc.org/cgi/doi/10.1074/jbc.M113.472654

23. Starck SR, Tsai JC, Chen K, Shodiya M, Wang L, Yahiro K, et al. Translation from the 5' untranslated region shapes the integrated stress response. Science [Internet]. 2016 Jan 29 [cited 2016 Aug 17];351(6272):aad3867. Available from: http://www.ncbi.nlm.nih.gov/pubmed/26823435

24. Andreev DE, O'Connor PBF, Zhdanov A V, Dmitriev RI, Shatsky IN, Papkovsky DB, et al. Oxygen and glucose deprivation induces widespread alterations in mRNA translation within 20 minutes. Genome Biol [Internet]. 2015 Dec 6 [cited 2016 Aug 17];16(1):90. Available from: http://genomebiology.com/2015/16/1/90

25. Shalgi R, Hurt JA, Krykbaeva I, Taipale M, Lindquist S, Burge CB. Widespread Regulation of Translation by Elongation Pausing in Heat Shock. Mol Cell. 2013;49(3):439–52.

26. Wiita AP, Ziv E, Wiita PJ, Urisman A, Julien O, Burlingame AL, et al. Global cellular response to chemotherapy-induced apoptosis. Elife [Internet]. 2013 Jul [cited 2016 Aug 17];2(1):e01236. Available from: http://linkinghub.elsevier.com/retrieve/pii/S1097276507004005

27. Gerashchenko M V., Lobanov A V., Gladyshev VN. Genome-wide ribosome profiling reveals complex translational regulation in response to oxidative stress. Proc Natl Acad Sci [Internet]. 2012 Oct 23 [cited 2016 Aug 17];109(43):17394–9. Available from: http://www.pnas.org/cgi/doi/10.1073/pnas.1120799109

28. Liu B, Han Y, Qian S-B. Cotranslational Response to Proteotoxic Stress by Elongation Pausing of Ribosomes. Mol Cell. 2013;49(3):453–63.

29. Mackowiak SD, Zauber H, Bielow C, Thiel D, Kutz K, Calviello L, et al. Extensive identification and analysis of conserved small ORFs in animals. Genome Biol [Internet]. 2015 Dec 14 [cited 2016 Aug 23];16(1):179. Available from: http://genomebiology.com/2015/16/1/179

30. Andrews SJ, Rothnagel JA. Emerging evidence for functional peptides encoded by short open reading frames. Nat Rev Genet [Internet]. 2014 Mar [cited 2016 Aug 17];15(3):193–204. Available from: http://www.ncbi.nlm.nih.gov/pubmed/24514441

31. Oyama M, Itagaki C, Hata H, Suzuki Y, Izumi T, Natsume T, et al. Analysis of Small Human Proteins Reveals the Translation of Upstream Open Reading Frames of mRNAs. Genome

Res [Internet]. 2004 Oct 15 [cited 2016 Aug 17];14(10b):2048–52. Available from: http://www.genome.org/cgi/doi/10.1101/gr.2384604

32. Selpi S, Bryant CH, Kemp GJ, Sarv J, Kristiansson E, Sunnerhagen P, et al. Predicting functional upstream open reading frames in Saccharomyces cerevisiae. BMC Bioinformatics [Internet]. 2009 [cited 2016 Aug 17];10(1):451. Available from: http://www.biomedcentral.com/1471-2105/10/451

33. Hu Q, Merchante C, Stepanova AN, Alonso JM, Heber S. Genome-Wide Search for Translated Upstream Open Reading Frames in Arabidopsis Thaliana. IEEE Trans Nanobioscience [Internet]. 2016 Mar [cited 2016 Aug 31];15(2):148–57. Available from: http://ieeexplore.ieee.org/lpdocs/epic03/wrapper.htm?arnumber=7404026

34. Fields AP, Rodriguez EH, Jovanovic M, Stern-Ginossar N, Haas BJ, Mertins P, et al. A Regression-Based Analysis of Ribosome-Profiling Data Reveals a Conserved Complexity to Mammalian Translation. Mol Cell. 2015;60(5):816–27.

35. Raj A, Wang SH, Shim H, Harpak A, Li YI, Engelmann B, et al. Thousands of novel translated open reading frames in humans inferred by ribosome footprint profiling. Elife [Internet]. 2016 [cited 2016 Aug 31];5. Available from: http://www.ncbi.nlm.nih.gov/pubmed/27232982

36. Harrow J, Frankish A, Gonzalez JM, Tapanari E, Diekhans M, Kokocinski F, et al. GENCODE: The reference human genome annotation for The ENCODE Project. Genome Res [Internet]. 2012 Sep 1 [cited 2016 Aug 21];22(9):1760–74. Available from: http://genome.cshlp.org/cgi/doi/10.1101/gr.135350.111

37. Alexandrov LB, Nik-Zainal S, Wedge DC, Aparicio SAJR, Behjati S, Biankin A V., et al. Signatures of mutational processes in human cancer. Nature [Internet]. 2013 Aug 14 [cited 2016 Aug 17];500(7463):415–21. Available from: http://www.nature.com/doifinder/10.1038/nature12477

38. McVean GA, Altshuler (Co-Chair) DM, Durbin (Co-Chair) RM, Abecasis GR, Bentley DR, Chakravarti A, et al. An integrated map of genetic variation from 1,092 human genomes. Nature [Internet]. 2012 Oct 31 [cited 2016 Aug 17];491(7422):56–65. Available from: http://www.nature.com/doifinder/10.1038/nature11632

39. Wen Y, Liu Y, Xu Y, Zhao Y, Hua R, Wang K, et al. Loss-of-function mutations of an inhibitory upstream ORF in the human hairless transcript cause Marie Unna hereditary hypotrichosis. Nat Genet [Internet]. 2009 Feb 4 [cited 2016 Aug 31];41(2):228–33. Available from: http://www.nature.com/doifinder/10.1038/ng.276

40. Raveh-Amit H, Maissel A, Poller J, Marom L, Elroy-Stein O, Shapira M, et al. Translational Control of Protein Kinase C by Two Upstream Open Reading Frames. Mol Cell Biol [Internet]. 2009 Nov 15 [cited 2016 Aug 31];29(22):6140–8. Available from: http://mcb.asm.org/cgi/doi/10.1128/MCB.01044-09

41. Fayyad U, Irani K. Multi-Interval Discretization of Continuous-Valued Attributes for Classification Learning. donga.ac.kr [Internet]. [cited 2016 Aug 17]; Available from: http://web.donga.ac.kr/kjunwoo/files/Multi interval discretization of continuous valued attributes for classification learning.pdf

42. Liu B, Dai Y, Li X, Lee WS, Yu PS. Building text classifiers using positive and unlabeled examples. In: Third IEEE International Conference on Data Mining [Internet]. IEEE Comput. Soc; 2003 [cited 2016 Aug 17]. p. 179–86. Available from: http://ieeexplore.ieee.org/lpdocs/epic03/wrapper.htm?arnumber=1250918

43. Battle A, Khan Z, Wang SH, Mitrano A, Ford MJ, Pritchard JK, et al. Genomic variation. Impact of regulatory variation from RNA to protein. Science [Internet]. 2015 Feb 6 [cited 2016 Aug 31];347(6222):664–7. Available from: http://www.ncbi.nlm.nih.gov/pubmed/25657249

44. Gene Ontology Consortium T, Ashburner M, Ball CA, Blake JA, Botstein D, Butler H, et al. Gene Ontology: tool for the unification of biology.

45. Author T, Benjamini Y, Hochberg Y, Benjaminit Y. Controlling the False Discovery Rate: A Practical and Powerful Approach to Multiple Controlling the False Discovery Rate: a Practical and Powerful Approach to Multiple Testing. Source J R Stat Soc Ser B J R Stat Soc Ser B J R Stat Soc B [Internet]. 1995 [cited 2016 Aug 31];57(1):289–300. Available from: http://www.jstor.org/stable/2346101

46. Maere S, Heymans K, Kuiper M. BiNGO: a Cytoscape plugin to assess overrepresentation of Gene Ontology categories in Biological Networks. Bioinformatics. 2005;21(16):3448–9.

47. Pontén F, Gry M, Fagerberg L, Lundberg E, Asplund A, Berglund L, et al. A global view of protein expression in human cells, tissues, and organs. Mol Syst Biol [Internet]. 2009 Dec 22 [cited 2016 Aug 17];5(1):799–816. Available from: http://msb.embopress.org/cgi/doi/10.1038/msb.2009.93

48. Wethmar K, Schulz J, Muro EM, Talyan S, Andrade-Navarro MA, Leutz A. Comprehensive translational control of tyrosine kinase expression by upstream open reading frames. Oncogene [Internet]. 2016 Mar 31 [cited 2016 Aug 17];35(13):1736–42. Available from: http://www.nature.com/doifinder/10.1038/onc.2015.233

Figures:

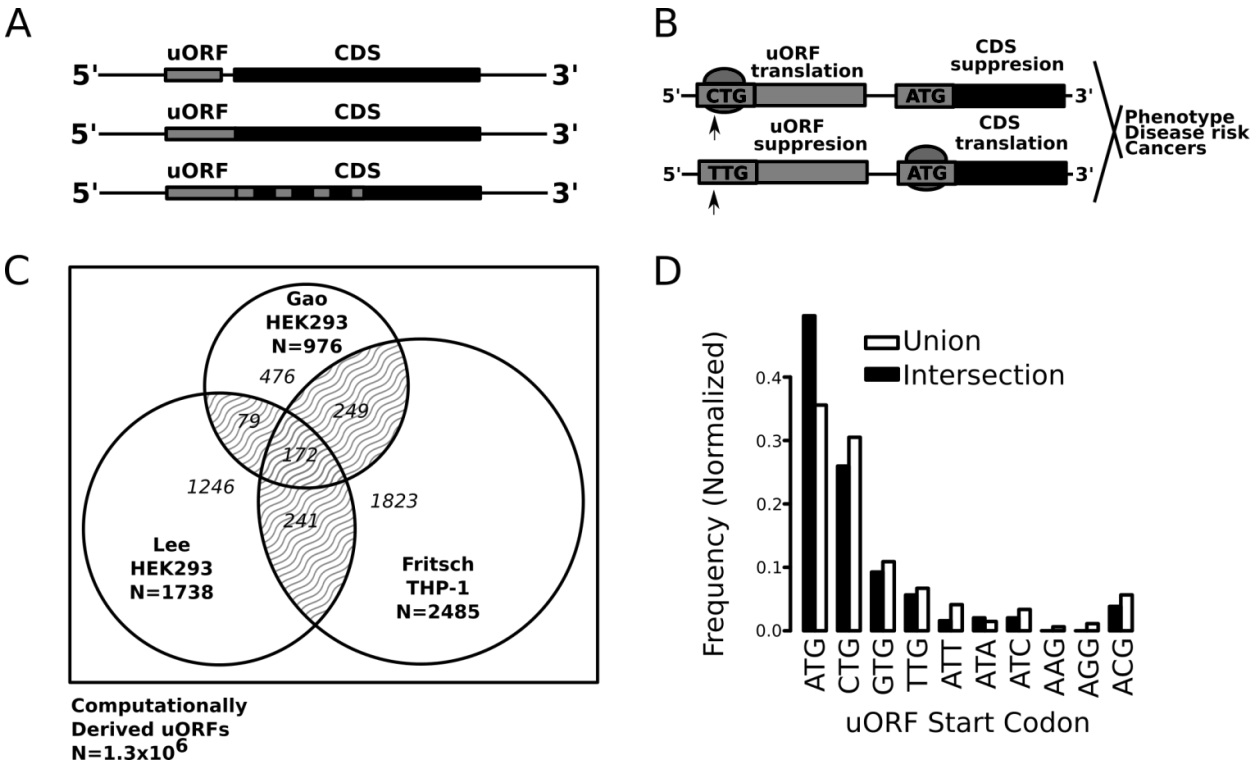

Figure 1:

A. ***The structure of upstream open reading frames.*** The stop codon for a uORF may be located before the CDS start codon. It may also be located within the CDS, if the uORF is frame-shifted relative to the CDS (upper and middle, respectively). An open reading frame may also utilize the same stop codon as the CDS, such that the ORF acts as a 5' extension of the CDS.

B. ***The effect of mutation or variation on upstream open reading frames.*** The creation or destruction of an upstream open-reading, may result in downstream effect on the rate of translation of the coding sequence. Change in degree of translation of the coding sequence, may in turn, result in change in phenotype, and disease risk.

C. ***The global space of upstream open reading frames, and within that space, the subset of ribosome profiling identified uORFs.*** Ribosome studies by Fritsch et al., Lee et al., and Gao et al., are interpreted as a Venn diagram. Pair-wise and three-way intersections between these experiments are highlighted, as these uORFs consititute our gold standard positive set. The universe of all possible uORFs, is derived from the GENCODE annotation, and numbers 1.3 million. Ribosome profiling positive uORFs, are used to identify a population of predicted positive uORFs, among the set of 1.3 million computationally derived uORFs.

D. The frequence of uORF ATG start codons, and near-cognate start codons, from ribosome profiling experiments. Frequency is given both for the overall frequency of start codons (union), and uORFs that are translated in more than one experiment (intersection).

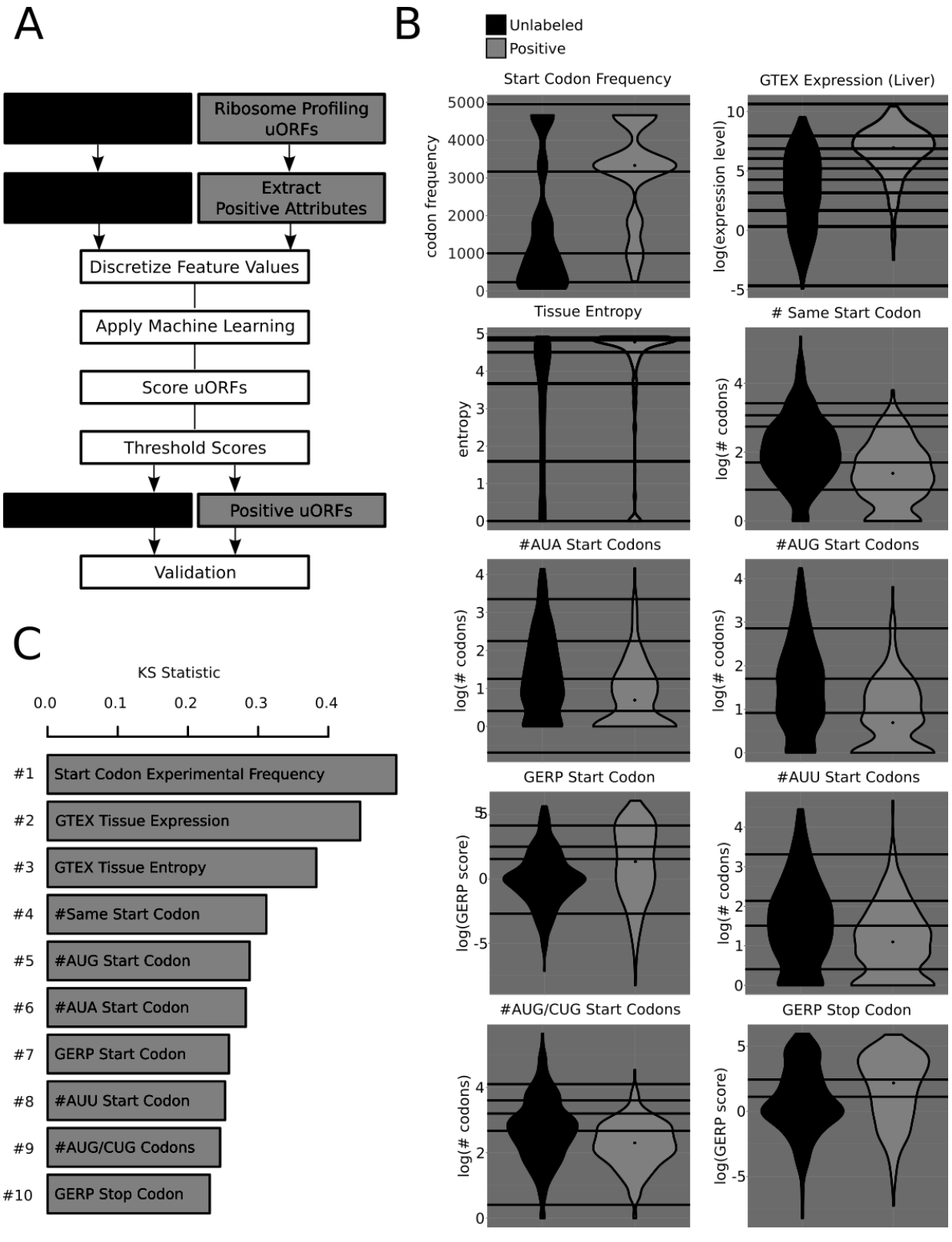
A
Ribosome Profiling uORFs
Extract Positive Attributes
Discretize Feature Values
Apply Machine Learning
Score uORFs
Threshold Scores
Positive uORFs
Validation
B
Unlabeled
Positive
Start Codon Frequency
codon frequency
GTEX Expression (Liver)
log(expression level)
Tissue Entropy
entropy
# Same Start Codon
log(# codons)
#AUA Start Codons
#AUG Start Codons
GERP Start Codon
log(GERP score)
#AUU Start Codons
#AUG/CUG Start Codons
GERP Stop Codon
C
KS Statistic
0.0
0.1
0.2
0.3
0.4
#1 Start Codon Experimental Frequency
#2 GTEX Tissue Expression
#3 GTEX Tissue Entropy
#4 #Same Start Codon
#5 #AUG Start Codon
#6 #AUA Start Codon
#7 GERP Start Codon
#8 #AUU Start Codon
#9 #AUG/CUG Codons
#10 GERP Stop Codon

Figure 2:

A. ***Methodology for distinguishing positive from unlabeled uORFs.*** Computationally derived uORFs and ribosome profiling identified uORFs, represent unlabeled and positive examples respectively. Attributes of these positive and unlabeled uORFs are extracted. The positive and unlabeled examples are used to train a machine learning algorithm. The machine learning algorithm assigns a score all computationally derived uORFs. A threshold on this score, yields positive and negative uORFs.

B. ***Distributions of attributes for positive and unlabeled uORFs.*** The attributes of uORF, are used to distinguish positive from unlabeled uORFs. Attributes like the sequence conservation (GERP score), and tissue mRNA expression (GTEX Expression - Liver), have different continuous distributions for the unlabeled uORFs, compared to the positive uORFs. These continuous distributions, can be discretized and optimized for machine learning, using the minimum description length principle (MDLP) binning algorithm. Horizontal lines on the plot correspond to these binning intervals. The 10 attributes with the greatest difference in distribution (largest kolmogorov smirnov statistic) between positive and unlabeled uORFs are shown.

C. Upstream open reading frame attributes as classifiers, ranked. The kolmogorov smirnov (KS) test provides an index for distinction between positive and unlabeled attributes. Attributes are ranked, according to the difference in distribution between positive and unlabeled attributes, using the KS statistic. The KS statistic thus provides an index for the utility of attributes in distinguishing between positive and unlabeled uORFs.

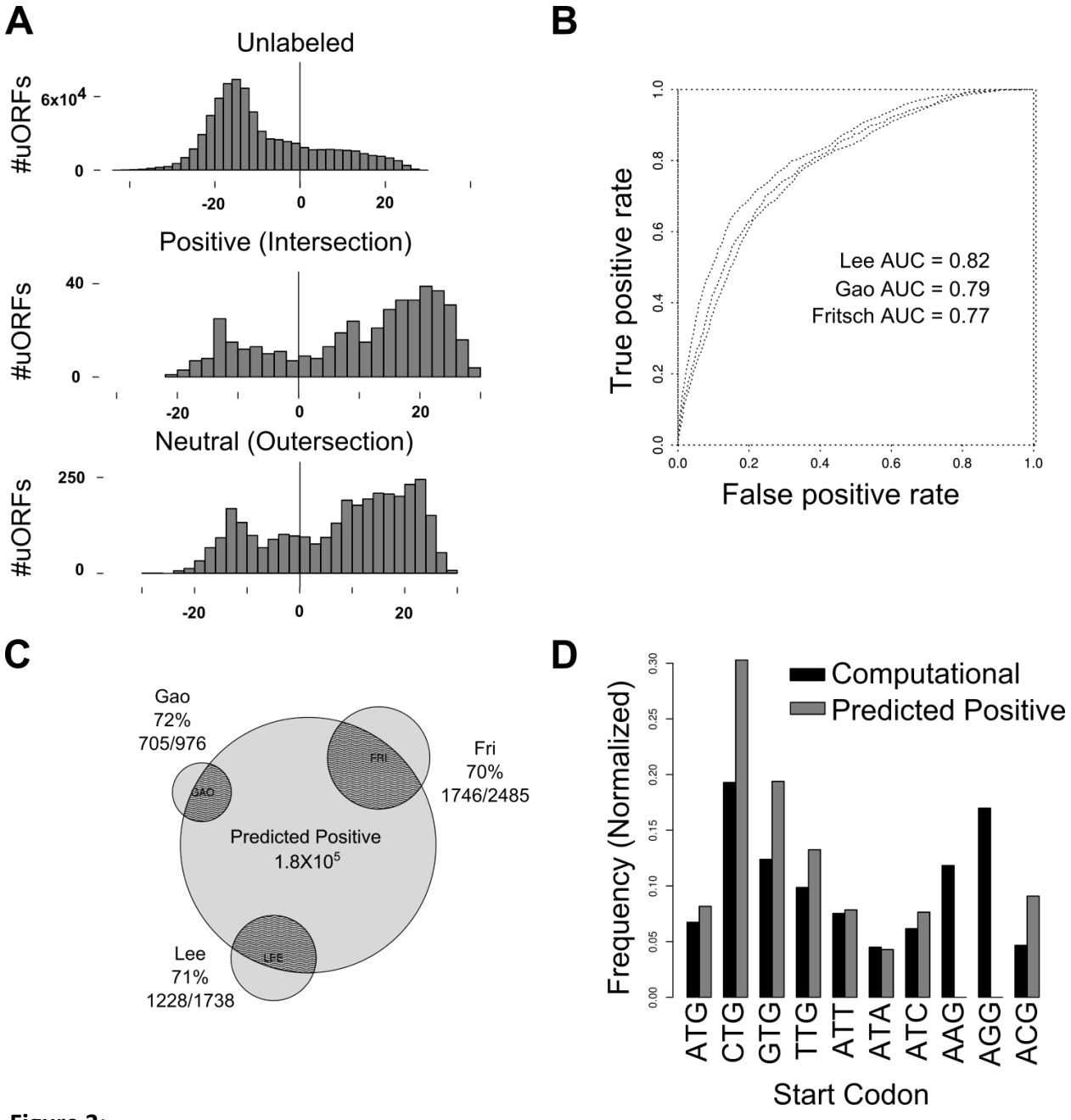

Figure 3:

A. Score distributions for upstream open reading frames, according to category determined via ribosome profiling. Score distributions for [a] and unlabeled uORFs, that are identified computationally, through a comprehensive scan of the GENCODE annotation, but are not found translated in any ribosome profiling experiment (top), [b] positive ribosome profiling uORFs, that are positively identified in two or more ribosome profiling experiments (middle), and [c] neutral ribosome profiling uORFs, that are identified in only a single ribosome profiling experiment, and are so witheld from both the positive and the unlabeled sets (bottom).
B. ROC curves gauge performance of the machine learning algorithm. The machine learning algorithm was trained on two of the three ribosome profiling data set, and then used to extract

the third data set from the unlabeled data set. The ROC curve is shown for each of the three combinations 1. Train Lee et al. and Fritsch et al. – extract Gao et al. (AUC = 0.79), 2. Train Lee et al. and Gao et al. – extract Fritsch et al. (AUC = 0.77). 3. Train Fristch et al. and Gao et al. - extract Lee et al. (AUC = 0.82).

C. Positively identifed uORFs from the computational set, and ribosome profiling experiments. Of the computationally derived uORFs extracted from the GENCODE annotation, approximately 180 000 are predicted as active upstream open reading frames. These are the upstream open reading frames that are predicted to undergo translation. This large set, includes 72% of the uORFs identified in the ribosome profiling experiment of Gao et al., 71% of the uORFs identified in the experiment of Lee et al., and 70% of the uORFs identified in the experiment of Fritsch et al.

D. The frequence of uORF ATG start codons, and near-cognate start codons, for predicted positive upstream open reading frames. Frequency is given both for the overall frequency of computationally derived uORFs from GENCODE (computational), and for the subset of computationally derived uORFs that are predicted to be translated (predicted positive).

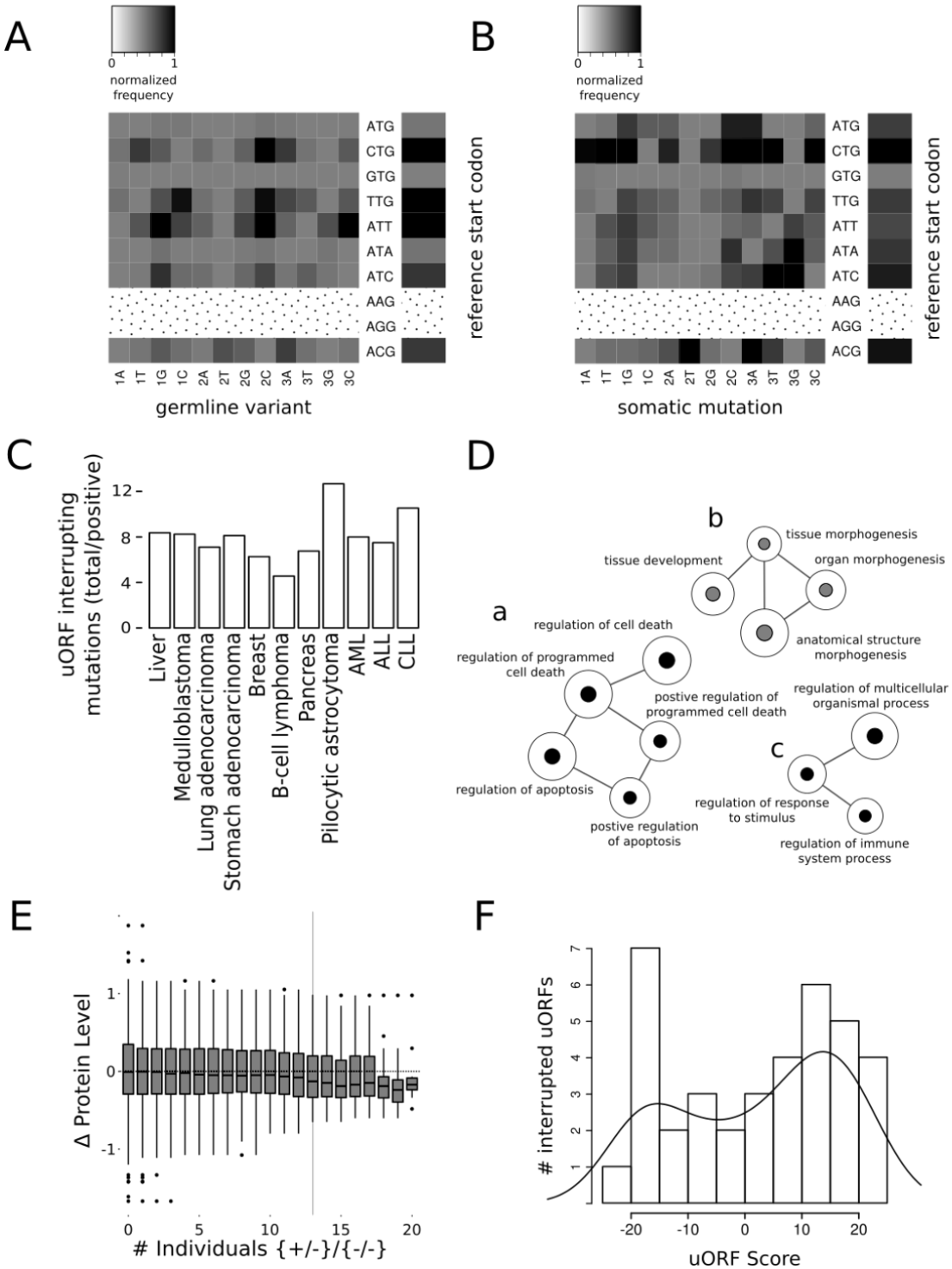
A
normalized frequency
ATG
CTG
GTG
TTG
ATT
ATA
ATC
AAG
AGG
ACG
reference start codon
1A 1T 1G 1C 2A 2T 2G 2C 3A 3T 3G 3C
germline variant
B
somatic mutation
C
uORF interrupting mutations (total/positive)
Liver
Medulloblastoma
Lung adenocarcinoma
Stomach adenocarcinoma
Breast
B-cell lymphoma
Pancreas
Pilocytic astrocytoma
AML
ALL
CLL
D
tissue morphogenesis
tissue development
organ morphogenesis
anatomical structure morphogenesis
regulation of cell death
regulation of programmed cell death
postive regulation of programmed cell death
regulation of multicellular organismal process
regulation of apoptosis
postive regulation of apoptosis
regulation of response to stimulus
regulation of immune system process
E
Δ Protein Level
Individuals {+/-}/{-/-}
F
interrupted uORFs
uORF Score

Figure 4:

A: Density matrix, showing the distribution of 1000 genomes variants, interrupting postively scored uORF start codons. The vertical axis displays the reference start codon, the horizontal axis shows the interrupting variant (position – 1,2,3 – and codon – A,T,G,C).
B: Density matrix, showing the distribution somatic mutations found in tumor samples (Alexandrov et al.), interrupting positively scored uORF start codons. The vertical axis displays the reference start codon, the horizontal axis shows the interrupting variant (position – 1,2,3 – and codon – A,T,G,C).
C: Ratio of all uORFs interrupted by start-codon destroying mutants (Alexandrov et al.), to positively scored uORFs interrupted by start codon destroying mutants, according to cancer type.
D: GO/PANTHER terms, for statistically overrepresented genes with uORF start codons interrupted by somatic variants in tumor samples (Alexandrov et al.). The size of each node, corresponds to the number of uORFs associated that GO term. Thresholds were established to eliminate relatively common GO terms (>1250 associated uORFs), and relatively uncommon GO terms (<250 associated uORFs). This was done, in order to produce a network structure that is neither too general, nor too specific. 3 principle networks emerge a) tissue morphogenesis b) immune function c) apoptosis. Networks were developed using the statistical package BiNGO, and include adjustment for multiple testing.
E: The standardized change in protein level for a given gene, between wild type individuals, and individuals with uORF start codon interrupting variants. This difference in protein level is shown for different ratios of variant possessing individuals (+/-, -/-) to wild-type individuals (+/+). Larger numbers of individuals with the variant allele, allow for larger statistical power, in calculating the effect of the variant on protein level.
F: rQTLs (Battle et al. 2015) interrupting uORF start codons, according to the score of the corresponding uORF. rQTLs are more likely to be associated with a positive scoring uORF.

Tables:

Table 1: uORF features. Features are listed according to the KS statistic for each attribute, measured between positive and unlabeled uORFs.

Rank	***Attribute***	***KS statistic***	***p value***	***Rank***	***Attribute***	***KS statistic***	***p value***
1	GTEX Bone Marrow	0.54	0.000	46	#AGG	0.20	0.000
2	GTEX Liver	0.50	0.000	47	#CTG	0.20	0.000
3	GTEX Lung	0.49	0.000	48	Kozak context	0.19	0.000

4	GTEX Pituitary	0.49	0.000	49	% GERP elements	0.19	0.000
5	Ribosome profiling uORF start codon frequency	0.48	0.000	50	uORF start codon to CDS start codon distance	0.19	0.000
6	GTEX Nerve	0.48	0.000	51	mRNA ΔG uORF start [20-59]BP	0.18	0.000
7	GTEX Muscle	0.47	0.000	52	#GTG	0.18	0.000
8	GTEX Pancreas	0.47	0.000	53	mRNA ΔG uORF start [40-79]BP	0.18	0.000
9	GTEX Adipose Tissue	0.47	0.000	54	%A	0.17	0.000
10	GTEX Skin	0.47	0.000	55	5' cap to uORF start codon distance	0.16	0.000
11	GTEX Spleen	0.47	0.000	56	mRNA ΔG uORF stop codon [0,39]BP	0.16	0.000
12	GTEX Stomach	0.46	0.000	57	mRNA ΔG uORF stop codon [-20,19]BP	0.16	0.000
13	GTEX Cervix Uteri	0.46	0.000	58	uORF stop codon to CDS start codon distance	0.16	0.000
14	***GTEX (combined)***	***0.46***	***0.000***	59	mRNA ΔG CDS start [-20,19]BP	0.14	0.000
15	GTEX Salivary Gland	0.46	0.000	60	Noderer context	0.13	0.000
16	GTEX Uterus	0.46	0.000	61	%G	0.13	0.000
17	GTEX Small Intestine	0.46	0.000	62	mRNA ΔG uORF start [60,99]BP	0.12	0.000
18	GTEX Prostate	0.46	0.000	63	mRNA ΔG uORF start [80,119]BP	0.12	0.000

19	GTEX Esophagus	0.46	0.000	64	mRNA ΔG uORF start [-20,19]BP	0.12	0.000
20	GTEX Heart	0.46	0.000	65	mRNA ΔG uORF end [-40,-1]	0.11	0.000
21	GTEX Bladder	0.46	0.000	66	mRNA ΔG uORF start [100,139]	0.11	0.000
22	GTEX Brain	0.45	0.000	67	mRNA ΔG CDS start [20,59]	0.11	0.000
23	GTEX Breast	0.45	0.000	68	mRNA ΔG uORF start [0,39]	0.10	0.000
24	GTEX Blood Vessel	0.45	0.000	69	%C	0.10	0.000
25	GTEX Fallopian Tube	0.45	0.000	70	mRNA ΔG uORF end [20,59]	0.09	0.000
26	GTEX Blood	0.45	0.000	71	mRNA ΔG CDS start [40,79]	0.09	0.000
27	GTEX Thyroid	0.44	0.000	72	mRNA ΔG uORF end [40,79]	0.08	0.000
28	GTEX Vagina	0.44	0.000	73	SNPs/length	0.07	0.001
29	GTEX Colon	0.44	0.000	74	mRNA ΔG CDS start [0,39]	0.06	0.004
30	GTEX Kidney	0.43	0.000	75	#TCG	0.06	0.011
31	GTEX Testis	0.43	0.000	76	mRNA ΔG CDS start 100.139	0.05	0.027
32	GTEX Adrenal Gland	0.42	0.000	77	mRNA ΔG uORF start [80,119]	0.05	0.028
33	GTEX Ovary	0.41	0.000	78	%T	0.05	0.053
34	GTEX Tissue Entropy	0.40	0.000	79	#ACG	0.05	0.056
35	#Same start codon	0.30	0.000	80	#CGA	0.04	0.142

36	#ATG	0.28	0.000	81	#CGT	0.04	0.198
37	#ATA	0.28	0.000	82	mRNA ΔG CDS start [60,99]	0.03	0.309
38	#ATT	0.26	0.000	83	uORF length (BP)	0.03	0.447
39	#ATG + CTG	0.26	0.000	84-89	#ACG		
40	#AAG	0.23	0.000	84-89	#CTA		
41	#ATC	0.22	0.000	84-89	#GTA		
42	Size 5'UTR (%)	0.22	0.000	84-89	Heterozygosity/length		
43	Start codon GERP score	0.22	0.000	84-89	#1000 Genomes SNPs		
44	Stop codon GERP score	0.21	0.000	84-89	Heterozygosity		
45	#TTG	0.21	0.000				

Table 3: Individual genes, with uORFs interrupted by germline human variation. Top 10, with disease assocations.

uORF ID	***SNP***	***Score***	***VAF***	***Gene***	***Transcripts Affected***	***Disease Process (PMID)***
ENST00000435422.3.uORF_CTG.11	rs13170573	12.3	0.47	SGCD	28/80	OSA (25474115)
ENST00000526686.1.uORF_TTG.4	rs1461496	10.3	0.68	HSPA8	3/72	CHF/asthma (20300519, 22370858)
ENST00000228872.4.uORF_CTG.8	rs34330	21.5	0.66	CDKN1B	4/9	Various cancers (17908995)
ENST00000355739.4.uORF_ATG.13	rs751402	15.0	0.71	ERCC5	3/45	Gastric cancer (27228234)
ENST00000302418.4.uORF_ACG.1	rs12251445	23.9	0.31	KIF5B	1/7	Exercise response (18984674)

ENST00000270139.3.uORF_GTG.2	rs2850015	24.2	0.78	IFNAR1	2/16	Malaria susceptibility (25445652)
ENST00000270139.3.uORF_GTG.4	rs2850015	23.1	0.78	IFNAR1	2/16	
ENST00000406438.3.uORF_ATT.1	rs1563634	9.0	0.68	SMCR8	1/3	Cancer risk (19432957)
ENST00000462284.1.uORF_ATC.1	rs937283	19.2	0.34	MDM2	15/20	Epithelial cancer (26261649)
ENST00000310823.3.uORF_CTG.2	rs12692386	21.5	0.58	ADAM17	4/8	Vascular disease (24853957)

Table 4: Individual genes, with uORFs interrupted by somatic cancer mutations. Top 10 by prediction score.

uORF ID	Location	Score	Cancer Type	Gene Name	Transcripts Affected
ENST00000371142.4.uORF_ACG.2	98346749	28.4	Lung	TM9SF3	2/3
ENST00000371142.4.uORF_ACG.1	98346749	28.1	Lung	TM9SF3	2/3
ENST00000254480.5.uORF_ACG.2	47823347	26.9	Lung	SMARCC1	3/8
ENST00000254480.5.uORF_ACG.1	47823347	26.8	Lung	SMARCC1	3/8
ENST00000000233.5.uORF_ACG.2	127228421	26.7	Stad	ARF5	1/3
ENST00000250894.4.uORF_ACG.1	1756190	26.5	Lung	MAPK8IP3	1/3
ENST00000345496.2.uORF_CTG.3	46221698	25.7	Breast	UBE2G2	4/15

ENST00000358015.3.uORF_GTG.2	110045592	25.6	Stad	RAD23B	2/17
ENST00000258341.4.uORF_ACG.1	182992786	25.5	Lung	LAMC1	1/8
ENST00000395686.3.uORF_GTG.1	53162310	25.4	Breast	ERO1L	5/20